



Article

# Removal of Polycyclic Aromatic Hydrocarbons in a Heterogeneous Fenton Like Oxidation System Using Nanoscale Zero-Valent Iron as a Catalyst

Tahir Haneef<sup>1</sup>, Muhammad Raza Ul Mustafa<sup>1,2,\*</sup> , Kashif Rasool<sup>3,\*</sup>, Yeek Chia Ho<sup>1,2</sup>  and Shamsul Rahman Mohamed Kutty<sup>1,2</sup>

<sup>1</sup> Department of Civil and Environmental Engineering, Universiti Teknologi PETRONAS, Seri Iskandar 32610, Perak, Malaysia; tahirhanifuaf@gmail.com (T.H.); yeekchia.ho@utp.edu.my (Y.C.H.); shamsulrahman@utp.edu.my (S.R.M.K.)

<sup>2</sup> Centre for Urban Resource Sustainability, Institute of Self-Sustainable Building, Universiti Teknologi PETRONAS, Seri Iskandar 32610, Perak, Malaysia

<sup>3</sup> Qatar Environment and Energy Research Institute (QEERI), Hamad Bin Khalifa University (HBKU), P.O. Box 5825, Doha, Qatar

\* Correspondence: raza.mustafa@utp.edu.my (M.R.U.M.); krasool@hbku.edu.qa (K.R.)

Received: 19 June 2020; Accepted: 23 July 2020; Published: 29 August 2020



**Abstract:** Oil and gas effluents contains highly toxic and harmful organic pollutants. Therefore, it is necessary to eliminate and/or reduced the concertation of organic pollutants to a technologically acceptable levels before their discharge into water streams. This study investigates the application of nanoscale zero-valent iron (nZVI), and hydrogen peroxide (H<sub>2</sub>O<sub>2</sub>) for removal of organic pollutants from real oily produced water. Batch studies were performed and effect of different operating parameters, including concentration of nZVI and H<sub>2</sub>O<sub>2</sub>, pH and reaction time were studied. Moreover, optimization of independent variables was performed using central composite design (CCD) in response surface methodology (RSM). The experimental set up provided maximum removal efficiencies of 89.5% and 75.3% for polycyclic aromatic hydrocarbons (PAHs) and chemical oxygen demand (COD), respectively. The optimum values of independent variables such as concentrations of nZVI, and H<sub>2</sub>O<sub>2</sub>, contact time and pH were obtained as 4.35 g/L, 1.60 g/L, 199.9 min and 2.9, respectively. Predicted PAHs and COD removal efficiencies at the optimum values of independent variables were found as 89.3% and 75.7%, respectively which are in line with the experimental values. The study indicates that application of heterogeneous Fenton like oxidation system using nZVI as a catalyst is an efficient treatment method for removal of organic pollutants from real produced water.

**Keywords:** produced water; polycyclic aromatic hydrocarbon; COD; nanoscale zero-valent iron; response surface methodology

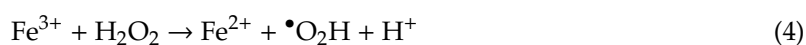
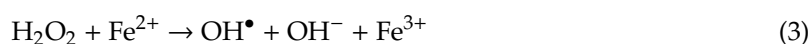
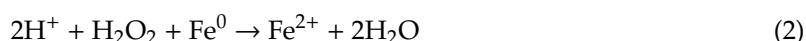
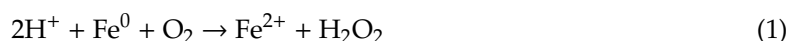
## 1. Introduction

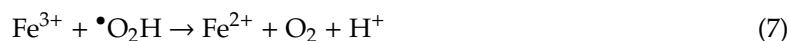
Oil and gas industries are one of the important sectors producing hazardous byproducts in the form of oily produced water [1]. Produced water is usually present in deep underground rocks and is brought to the ground surface during oil and gas extraction. Composition of produced water depends on the geological conditions of the site, type of hydrocarbons involved in extraction processes, characteristics of hydrocarbons well and extraction methods [2]. Produced water typically contains copious hazardous organic, inorganic pollutants, oxides, metals and minerals [3]. Globally, approximately 250 million barrel/per day produced water is generated from oil extraction processes [1,4], whereas in Malaysia, its production is about 1800 thousand barrel/per day [5].

Produced water contains high concentration of hazardous polycyclic aromatic hydrocarbons (PAHs) which are classified as low molecular weight (LMW) and high molecular weight (HMW) compounds based on number of benzene rings. For instance, naphthalene and acenaphthylene are LMW PAHs with two or three benzene rings, where HMW PAHs include pyrene and chrysene consisting of four or more fused benzene rings [4]. Acute and chronic toxicity of produced water is mainly assigned to presence of these PAHs, phenols and higher chemical oxygen demand (COD) concentrations [6]. Various physio-chemical and biological methods, such as electrocoagulation, membrane-based technologies, electrodialysis, ion exchange, adsorption and activated sludge processes have been employed for the treatment of produced water [5,7]. Nevertheless, these conventional treatment methods have many drawbacks, such as low removal efficiencies, high maintenance cost, more energy consumption, membrane fouling, and production of toxic byproducts [5].

Advanced oxidation processes (AOPs) has gained considerable attention recently as an alternative to conventional chemical methods to remove the refractory organic pollutants from wastewater [8]. Several AOPs have been employed for treatment of petroleum industry effluents. Among AOPs, homogeneous Fenton oxidation is considered one of the best options for remediation of these pollutants [9], as it can degrade an extensive range of organic micropollutants by producing hydroxyl radicals ( $\text{OH}^\bullet$ ) and can transform non-biodegradable organic pollutants into biodegradable substances [10]. However, production of a high amount of iron, toxic sludge and usage of significant amount of reagents limit the use of homogeneous Fenton oxidation [11].

Nowadays, heterogeneous Fenton like oxidation systems are being investigated by utilizing iron supported catalysts such as magnetite ( $\text{Fe}_3\text{O}_4$ ), zero-valent iron (ZVI), lepidocrocite ( $\gamma\text{-FeOOH}$ ) and goethite ( $\alpha\text{-FeOOH}$ ). However, except nanomaterials such as nanoscale ZVI (nZVI), many catalysts require ultraviolet (UV) radiation, visible irradiation, or ultrasound as additional assistance for remediation of pollutants [12]. Whereas nZVI has shown potential to address the issues discussed above because of its novel properties, cost-effectiveness, abundance in nature, and environmentally friendly nature [13]. The reduction potential of nZVI is  $E = -0.44$  V, which indicates it can effectively degrade wide range of refractory pollutants [14]. The nZVI rate of reaction is higher (up to 100 times) than other catalysts, such as conventional iron powders,  $\gamma\text{-FeOOH}$  and  $\text{Fe}_3\text{O}_4$  [15,16]. Zhang et al. [17] examined application of nZVI particles (size 1–100 nm) for degradation of organic pollutants and showed excellent reactivity of nZVI because of its large specific surface area ( $33.5 \text{ m}^2/\text{g}$ ). nZVI can be used as a catalyst in Fenton like oxidation system for the degradation of refractory organic pollutants. Heterogeneous Fenton like oxidation system using nZVI as a catalyst has been suggested for efficient degradation of organic contaminants in numerous studies [18]. In heterogeneous Fenton like oxidation system, nZVI generates  $\text{H}_2\text{O}_2$  by losing two-electron during reaction with  $\text{O}_2$ , as shown in Equation (1). The  $\text{OH}^\bullet$  radicals are also produced during the reaction of nZVI and  $\text{H}_2\text{O}_2$ , as presented in Equations (2) and (3). The  $\text{OH}^\bullet$  degrades organic pollutants via radical combination, electron transfer, and hydrogen abstraction, as shown in Equations (8)–(10), respectively [19]. While already produced  $\text{Fe}^{3+}$  ions may be reduced reacting with  $\text{H}_2\text{O}_2$  and regenerate  $\text{Fe}^{2+}$  ion, as shown in Equation (4). This mechanism known as Fenton like reaction, it allows regeneration of  $\text{Fe}^{2+}$  in an excellent cyclic process. Moreover, Equations (4)–(7) show the regeneration of  $\text{Fe}^{2+}$  from  $\text{Fe}^{3+}$  ion by consuming  $\text{H}_2\text{O}_2$  [20,21].





Response surface methodology (RSM) is a statistical and mathematical Design-Expert software which is commonly used for optimization purposes. It develops experimental design based on level of variables, which may help to minimize experimental work by providing optimal conditions [22]. In addition, it validates the interaction between independent and dependent factors [23]. Central composite design (CCD) is a standard, reliable, and accessible design in RSM. CCD improves statistical interpretations and gives fewer experimental runs with an overall experimental error [22].

Although heterogeneous Fenton like oxidation system using nZVI as a catalyst has been used for remediation of different pollutants in various wastewaters, such as groundwater [1], palm oil mill effluent [24], municipal wastewater [25], and metalworking fluids [26]. However, to date this has never been employed for PAHs removal from real oily produced water. Furthermore, no application of RSM has been observed which optimizes the combined PAHs and COD removal in produced water. Therefore, this work aims (i) to evaluate the potential of heterogeneous Fenton like oxidation system using nZVI as a catalyst for PAHs and COD removal from real produced water and (ii) to design experiments and evaluate optimal conditions of independent variables including, concentrations of nZVI and  $\text{H}_2\text{O}_2$ , pH and contact time using CCD and RSM.

## 2. Materials and Methods

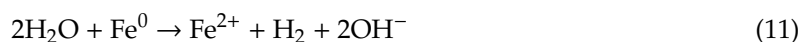
### 2.1. Materials

Produced water was collected from oil and gas exploration site in South East Asia region and stored at 4 °C following standard protocol prescribed by American Public Health Association (APHA) [27]. The analytical grade chemicals  $\text{H}_2\text{SO}_4$  (95–98%), NaOH (30% w/v), dichloromethane (DCM), acetonitrile and  $\text{H}_2\text{O}_2$  (30%) were purchased from R&M Chemicals Malaysia and utilized as received. A syringe filter with 0.45  $\mu\text{m}$  pore size (Whatman U.S.A, 25 mm dia) was used for filtration. Commercially available nZVI was used in this study without any surface modifications. The characterization of nZVI used was provided by manufacturer as more than 80% iron content, 50 nm particle size and 20–25  $\text{m}^2/\text{g}$  surface area. Many researchers have employed same nZVI (purchased from NANO IRON) for the treatment of copious types of wastewater and characterized using scanning electron microscope (SEM), X-ray diffraction (XRD) and transmission electron microscope (TEM). The results obtained were in line with the manufacturer's reported values. For instance, Taha et al. [24] characterized commercially available nZVI (from NANO IRON, Židlochovice, Czech Republic) using BET, SEM, XRD, TEM analysis and reported that pore size, surface area and size of nZVI were 6.18 nm,  $2.4 \times 10^{-5} \text{ m}^3/\text{kg}$ , and 49 nm respectively. Further, they accredited the existence of elemental iron (Fe) via XRD analysis. Energy dispersive X-ray (EDX) connected with SEM showed that surface of nZVI was comprised of Fe, carbon, oxygen and silicon. TEM image showed the presence of shell layer and core of nZVI [24]. Almost similar results of nZVI (from NANO IRON, Židlochovice, Czech Republic) characterization were reported by several other researchers [28–32]. Based on comprehensive literature review of commercially available nZVI (from NANO IRON, Židlochovice, Czech Republic), it is expected that nZVI used in current study may have similar characteristics to nZVI used in previous studies illustrated above.

### 2.2. Heterogeneous Fenton Like Oxidation System

Produced water sample of 300 mL was taken in a reactor (1 L glass beaker). The reactor was covered with an aluminum sheet to protect the water sample from sunlight. pH of produced water was adjusted using an appropriate volume of 1 M  $\text{H}_2\text{SO}_4$  and 1M NaOH solution. A known amount

of nZVI and H<sub>2</sub>O<sub>2</sub> were added to the water sample to initiate heterogeneous Fenton like oxidation reaction. A magnetic stirrer was used for homogeneous mixing. An increase in pH of reaction mixture was observed during the oxidation process due to reaction of nZVI with H<sub>2</sub>O<sub>2</sub> as shown in Equation (11) [33].



After a certain contact time, reaction was stopped by increasing pH of reaction mixture up to pH 10.

### 2.3. Produced Water Characterization

Total suspended solids (TSS) and five days biochemical oxygen demand (BOD<sub>5</sub>) was measured following the standard methods (APHA, 1992) [33]. Total organic carbon (TOC) was determined using TOC analyzer (TOC-VCSH, Shimadzu, Japan). COD analysis was performed using HACH method following U.S. Environmental Protection Agency (USEPA) method [1,34]. The presence of ferrous ions (Fe<sup>2+</sup>) in aqueous solution during COD analysis may interfere the COD value [35]. Therefore Fe<sup>2+</sup> ions were eliminated in the form of insoluble ferrous hydroxide (Fe(OH)<sub>2</sub>) by increasing pH of the aqueous solution up to pH 10. Treated produced water was centrifuged (Heraeus, MEGAFUGE 16-Centrifuge, Hanau, Germany) at 5000 rpm for 15 min to separate the insoluble Fe(OH)<sub>2</sub>. Finally, the supernatant was taken for COD and PAHs analysis. The COD and PAHs were calculated using Equations (12) and (13), respectively [36,37]. All experiments were performed in triplicate and average values were reported.

$$\text{COD (\%)} = \frac{\text{COD}_i - \text{COD}_f}{\text{COD}_i} \times 100 \quad (12)$$

$$\Sigma\text{PAHs (\%)} = \frac{\Sigma\text{PAHs}_i - \Sigma\text{PAHs}_f}{\Sigma\text{PAHs}_i} \times 100 \quad (13)$$

where in Equations (12) and (13) the subscripts “i” and “f” stand for initial and final concentration of COD and PAHs which were taken before and after treatment of produced water. Produced water samples for gas chromatography–mass spectrometry (GC-MS) analysis were prepared using liquid-liquid extraction (LLE) following USEPA method (3510C LLE) with few modifications. Briefly, 250 mL of produced water was taken in 500 mL separating funnel and 75 mL of DCM was added followed by vigorous shaking of about 5 min. The reaction mixture was kept at room temperature until a separate layer of aqueous and organics was formed [27]. Bottom organic phase was collected into a flask. The extraction was performed thrice using same aqueous layer and top supernatant was discarded. After mixing the three extracts into same flask, a calculated amount of anhydrous sodium sulfate was added into conical flask to absorb the water and then sample was filtered. The organic phase was concentrated up to 0.5 mL by rotary evaporator and transferred into 1.5 mL glass GC-MS vials and topped up using acetonitrile.

Prepared samples were analyzed via GC-MS (Agilent, model G7035A, combination of 7820A GC system with 5977E MSD, Santa Clara, CA, USA) with 30 m Elite 5MS column (inner diameter and film thickness were 0.25 mm and 0.25 μm, respectively) with helium as a carrier gas. The temperature of column was enhanced from 60 °C to 175 °C with 6 °C/min followed by the temperature of 240 °C with 3 °C/min and then finally held for 7 min at 300 °C. Temperature of injector and transfer line was 280 °C and 300 °C, in turn [1]. Identification was accomplished in selected ion monitoring (SIM) mode along with molecular masses of individual PAHs. A 16 PAHs mix standard solution with concentration of 2000 mg/L (Cat. No. 47930-U, Sigma Aldrich, Malaysia) was used for quantification of PAHs. The mixed standard solution was used by taking five-point calibration with a range from 10–300 μg/L. GC-MS chemstation software was utilized for assembling and treating the chromatographic data.

#### 2.4. Statistical Modelling and Design of Experiments Using Response Surface Methodology (RSM)

Statistical modelling and optimization of system was conducted by RSM and CCD based on Design-Expert software (Version 11, Stat-Ease, Minneapolis, MN, USA). RSM evaluated optimal values of independent parameters such as concentrations of nZVI (*A*), and H<sub>2</sub>O<sub>2</sub> (*B*), contact time (*C*) and pH (*D*). PAHs and COD removal was referred as responses. Performance of modelling technique was assessed by studying PAHs and COD removal efficiencies. For more straightforward statistical design, temperature and stirring speed were kept constant at 25–29 °C (room temperature) and 200 rpm, respectively to prevent from influence of other factors. All independent variables were changed into dimensionless codes, such as X<sub>1</sub> (nZVI concentration), X<sub>2</sub> (H<sub>2</sub>O<sub>2</sub> concentration), X<sub>3</sub> (contact time), and X<sub>4</sub> (pH) for comparison of variables with different units. It helps to reduce the error in statistical analysis (Equation (14)) [38].

$$XI = \frac{X_i - X_o}{\Delta X} \quad i = 1, 2, 3, \dots, k \quad (14)$$

In Equation (14), XI is the variable's coded values. While subscript "i" and "o" stand for *i*th value of independent parameter, and X<sub>i</sub> value at the center point, respectively. Whereas, ΔX is representing step change value. The ranges of variables like −1, 0 and +1 were designated to minimum, center and maximum level of variables according to the CCD principle, respectively. Ranges of all variables were finalized via preliminary experiments based on literature review. The CCD model levels (−1, 0 and +1) and all independent variables used in the current study are shown in Table 1.

**Table 1.** Actual and coded values for experimental design for the Fenton process.

Factors	Independent Variables	Coded Values			Star Point α = 1	
		−1	0	1	−α	+α
A	nZVI conc. (g/L)	1.0	3.50	6.0	1.0	6.0
B	Hydrogen peroxide (g/L)	0.4	1.625	2.85	0.4	2.85
C	Contact time (min)	30	115	200	30	200
D	pH	1.0	3.0	5.0	1.0	5.0

According to the principle of CCD, design consists of fractional factorial point (2<sup>k</sup>), axial point (2k) and center point (1). K represents total number of independent variables (4) defined earlier. Therefore, 30 experimental runs were conducted with fractional factorial point 16 (2<sup>4</sup>), axial point 8 (2 × 4) and central points (1). In addition, five replications of center point were performed for the final estimation of error. The values of experimental design are presented in Table 2. The behavior of experimental design was analyzed using CCD regression model which is represented by Equation (15) [39,40].

$$Y = b_0 + b_1A + b_2B + b_3C + b_4D + b_{12}AB + b_{13}AC + b_{14}AD + b_{23}BC + b_{24}BD + b_{34}CD + b_{11}A^2 + b_{22}B^2 + b_{33}C^2 + b_{44}D^2 \quad (15)$$

where *Y* is a predicted dependent variable and b<sub>0</sub>, b<sub>1</sub>, b<sub>2</sub>, b<sub>3</sub>, b<sub>4</sub>, b<sub>12</sub>, b<sub>13</sub>, b<sub>14</sub>, b<sub>23</sub>, b<sub>24</sub>, b<sub>34</sub>, b<sub>22</sub>, b<sub>33</sub> and b<sub>44</sub> are regression coefficients. *A*, *B*, *C* and *D* are independent variables that delineate linear effects, whereas, *AB*, *AC*, *AD*, *BC*, *BD*, and *CD*, are independent variables which describe interactive impact, while *A*<sup>2</sup>, *B*<sup>2</sup>, *C*<sup>2</sup> and *D*<sup>2</sup> show quadratic effect.

The quadratic regression Equation (15) can be used as a function of independent variables to predict the responses (PAHs and COD removal) and also can elucidate the interaction between independent parameters. The analysis of variance (ANOVA) interprets complicated relationship between independent and dependent factors of complete data. The model's significance is usually assessed by ANOVA results. Similarly, *R*-squared values of both models are also used for the confirmation of model significance [41]. In addition, sensitivity of four independent variables for PAHs and COD removal efficiencies are demonstrated by three dimensional (3D) plots.

**Table 2.** Experimental runs for PAHs and chemical oxygen demand (COD) removal.

Experiment No.	Independent Variables			
	nZVI Conc. (g/L)	H <sub>2</sub> O <sub>2</sub> Conc. (g/L)	Contact Time (min)	pH
1	6.0	2.85	200	1.0
2	6.0	0.40	30	1.0
3	3.5	1.62	115	3.0
4	3.5	2.85	115	3.0
5	3.5	1.62	115	3.0
6	3.5	1.62	115	3.0
7	1.0	2.85	200	1.0
8	3.5	1.62	115	3.0
9	3.5	0.40	115	3.0
10	3.5	1.62	200	3.0
11	1.0	0.40	200	1.0
12	6.0	1.62	115	3.0
13	1.0	2.85	30	1.0
14	1.0	2.85	30	5.0
15	3.5	1.62	115	1.0
16	6.0	2.85	30	5.0
17	3.5	1.62	30	3.0
18	1.0	0.40	30	5.0
19	6.0	0.40	30	5.0
20	3.5	1.62	115	3.0
21	3.5	1.62	115	5.0
22	6.0	2.85	200	5.0
23	1.0	0.40	200	5.0
24	6.0	2.85	30	1.0
25	1.0	1.62	115	3.0
26	3.5	1.62	115	3.0
27	1.0	2.85	200	5.0
28	6.0	0.40	200	5.0
29	1.0	0.40	30	1.0
30	6.0	0.40	200	1.0

### 3. Results and Discussion

#### 3.1. Produced Water Characteristics

Produced water contains large amount of organic and inorganic compounds resulting in higher concentrations of COD, TSS, turbidity and TOC. Therefore, characterization of water is important for designing an efficient treatment system. Table 3 depicts the characteristics of produced water used in this study.

**Table 3.** Characteristics of produced water.

Characteristics	Concentration (mg/L)
BOD	50.0
COD	2213.0
TSS	139
Turbidity	85 NTU
NH <sub>3</sub> -N	28.0
TOC	759.4

The COD and TOC concentrations of 2213 mg/L and 759.4 mg/L, respectively, indicate presence of higher number of organic compounds in produced water [42]. Figure 1 portrays characterization of 15 different PAHs compounds present in real produced water. Naphthalene was presented at highest

concentration of 201.46  $\mu\text{g/L}$  and benzo (g, h, i) perylene was in lowest concentration of 23.15  $\mu\text{g/L}$  as compared to other PAHs. Our results are in line with earlier studies where various researchers have reported PAHs and COD of produced water in the range of 124–1000  $\mu\text{g/L}$  and 1220–2600  $\text{mg/L}$ , respectively [43–46].

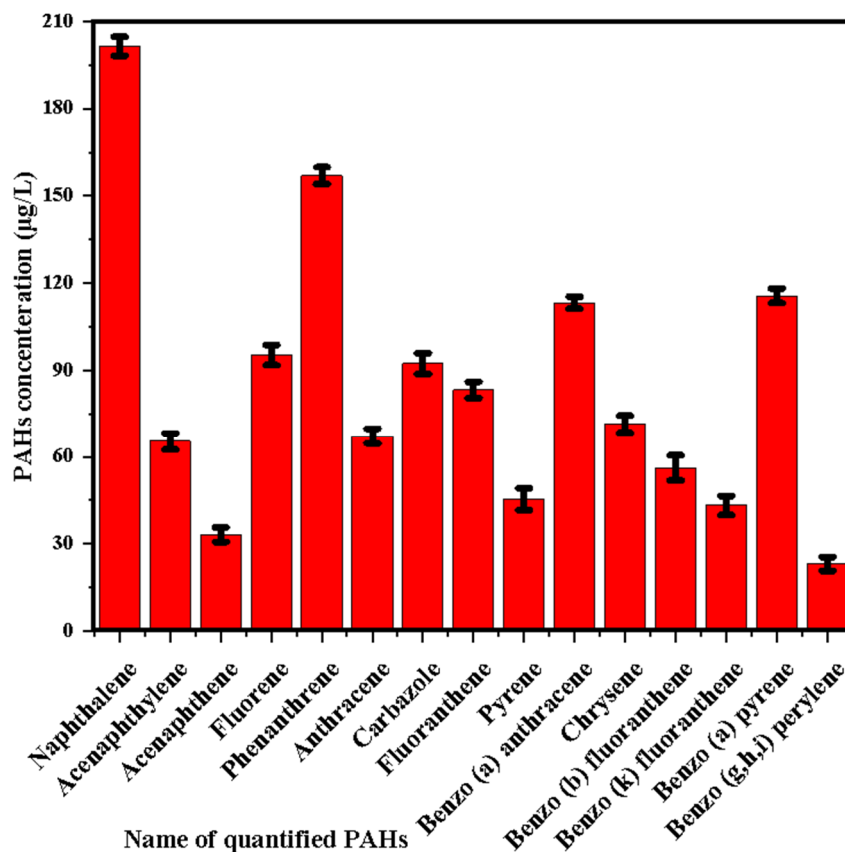


**Figure 1.** The concentration profiles of different polycyclic aromatic hydrocarbons (PAHs) characterized in real produced water.

### 3.2. Preliminary Batch Experiments

The preliminary experiments were conducted to optimize the operating parameters, such as concentrations of nZVI and  $\text{H}_2\text{O}_2$ , pH and contact time for COD removal. The nZVI was tested in range of 1.0 to 6.0  $\text{g/L}$  while keeping pH and contact time constant at 3.0 and 120 min, respectively. Initially, 32.4% of COD was reduced at 1.0  $\text{g/L}$  of nZVI. As the concentration of nZVI increased from 1.0  $\text{g/L}$  to 5.0  $\text{g/L}$ , removal efficiency of COD was also increased. The highest COD reduction of 53.5% was obtained at 5.0  $\text{g/L}$  of nZVI. Furthermore, at nZVI concentration higher than 5.0  $\text{g/L}$ , a decrease in COD removal was observed and at 6.0  $\text{g/L}$  of nZVI, COD removal efficiency reduced to 45.7%. The cause for this phenomenon may be linked to rise in the concentration of  $\text{Fe}^{2+}$  iron associated with nZVI concentration increment. Therefore, the increase in the concentration of  $\text{Fe}^{2+}$  led to enhance scavenging of  $\text{OH}^\bullet$  which led to the production of  $\text{Fe}^{3+}$  and  $\text{OH}^-$ . The  $\text{Fe}^{3+}$  iron and  $\text{OH}^-$  passivated the nZVI surface [47]. As a consequence, the  $\text{Fe}^{2+}$  iron substituted the refractory organic pollutants present in aqueous solution as the primary sink for  $\text{OH}^\bullet$ , leading to a significant reduction in degradation rate of organic pollutants at higher concentration [48]. Accordingly, 1.0–6.0  $\text{g/L}$  of nZVI was chosen for further analysis of PAHs and COD removal using CCD. Even though COD started to decline after 5.0  $\text{g/L}$  of nZVI concentration, 1.0  $\text{g/L}$  and 6.0  $\text{g/L}$  were selected as a maximum and minimum values for RSM, respectively, to design comprehensive experimental run.

The effect of  $H_2O_2$  was studied by changing the concentration in the range of 0.40 to 3.0 g/L while keeping pH, contact time and concentration of nZVI fixed at 3.0, 120 min and 5.0 g/L, respectively. At 0.5 g/L of  $H_2O_2$ , 45% of COD removal was obtained and it increased up to 71% at 2.0 g/L of  $H_2O_2$ . Further increases in  $H_2O_2$  concentration resulted in decreases in COD removal efficiencies. After investigating the impact of  $H_2O_2$  values on COD removal via screening test. It was noticed that a slight increase beyond 2.0 g/L of  $H_2O_2$  concentration decreased COD removal efficiencies. Thus, for comprehensive experimental design 0.40 g/L, and 2.85 g/L  $H_2O_2$  concentration was selected for RSM.

The effect of pH on COD removal was studied using pH values from pH 1.0 to pH 5.0 as shown in Figure 2c, while keeping the concentration of nZVI and  $H_2O_2$  fixed at 5.0 g/L and 2.0 g/L, respectively. The maximum COD removal of 71.2% was attained at pH 3.0. Further increase in pH resulted in reduction of COD removal efficiencies. Hence, pH 1.0 and 5.0 were chosen as a minimum and maximum values for Design Expert (CCD/RSM) to study pH influence on organic pollutants removal.

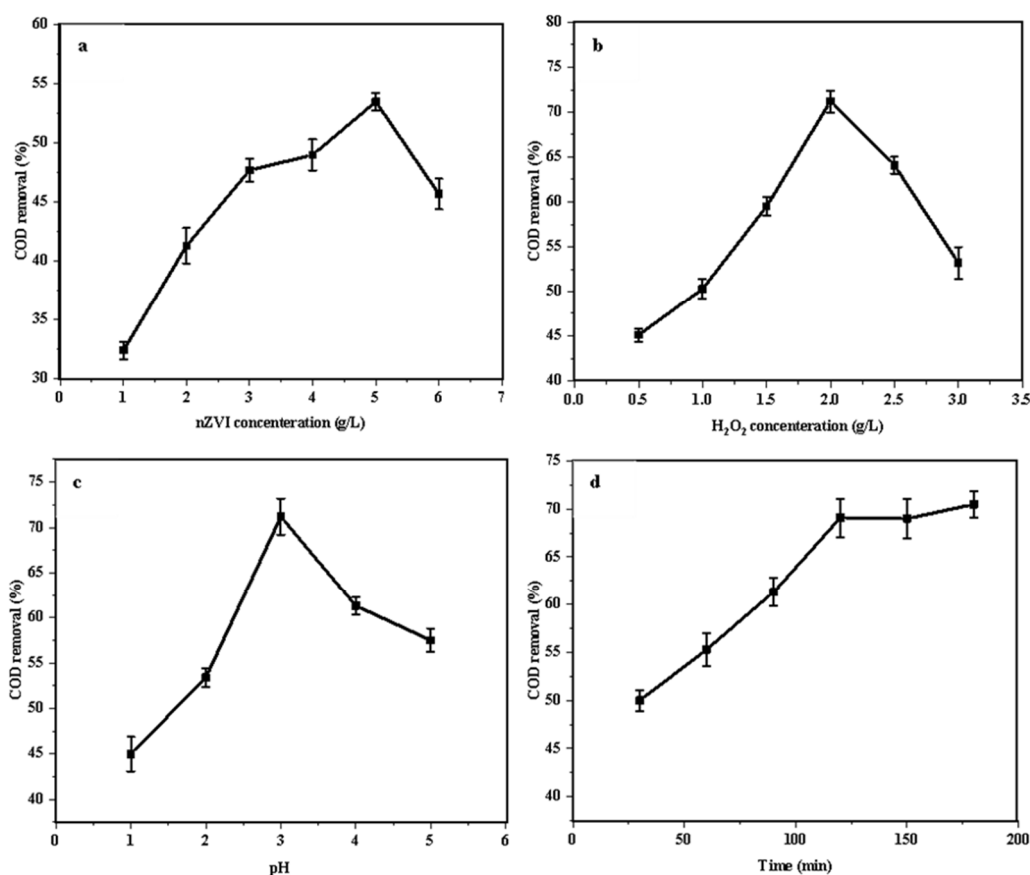


**Figure 2.** COD removal efficiencies at different concentrations of (a) nanoscale zero-valent iron (nZVI), (b)  $H_2O_2$ , (c) pH and (d) contact time.

The effect of contact time on COD removal was investigated from 30 to 200 min, while keeping all other operating parameters constant as shown in Figure 2d. Initially after 30 min of reaction time, 50% of COD removal was achieved. Contact time showed significant impact on organic oxidation and maximum COD removal of 70.5% was obtained at contact time of 200 min. No significant increase in COD removal was observed by increasing the contact time higher than 200 min. Thus, time ranges of 30 to 200 min were used for optimization purpose using Design-Expert software (Stat-Ease, Minneapolis, MN, USA). In all screening tests, the COD removal efficiency was considered as response factor (output) which evaluated the organic pollutant's degradation potential present in produced water. Based on the findings of organic pollutants removal, further tests were designed via RSM for the removal of PAHs and COD from produced water.



### 3.3. Batch Experiments Based on RSM Experimental Design

By performing batch experiments, the ranges of independent variables such as *A*, *B*, *C* and *D* were chosen for RSM optimization as shown in Table 1. These ranges of independent variables were utilized in CCD/RSM to design the experimental run for optimization work. CCD produced rotatable 30 experimental runs having different values of independent variables as shown in Table 2. All 30 sets of experiments proposed by CCD were performed in lab to study the removal of PAHs and COD for each set. The responses were predicted and the interaction between independent variables was also investigated using second order quadratic model as shown in Equations (16) and (17).

$$\text{COD removal efficiency (\%)} = 73.08 + 11.49A + 2.08B + 1.21C - 1.81D + 8.91AB - 1.28AC - 0.7812AD - 2.66BC - 1.41BD + 1.28CD - 12.40A^2 - 6.10B^2 - 0.4500C^2 - 18.60D^2 \quad (16)$$

$$\text{PAHs removal efficiency (\%)} = 85 + 7.53A - 3.79B + 3.34C - 3.93D + 5.78AB - 1.15AC - 0.100AD - 1.61BC - 3.99BD + 2.61CD - 11.78A^2 - 7.68B^2 + 0.17C^2 - 14.98D^2 \quad (17)$$

The experimental and predicted removal of PAHs and COD varied for each set of tests depending on different values of independent parameters. The maximum removal of PAHs (89.5%) and COD (76.3%) was observed in 10th experimental run, as depicted in Figure 3. The predicted and experimental values of all responses were in good agreement.

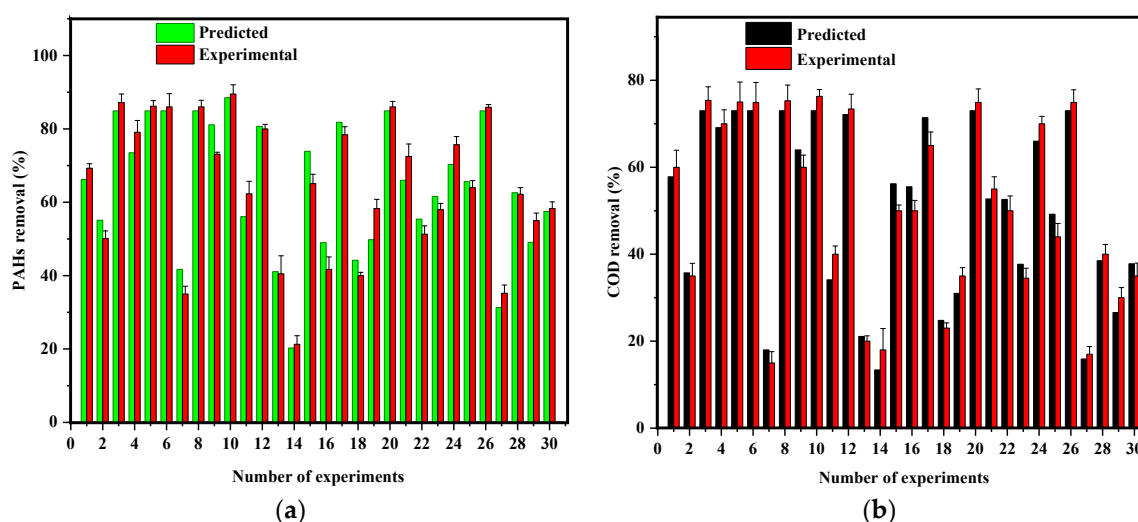


**Figure 3.** PAHs and COD removal against each set of experimental runs. (a) Predicted and experimental PAHs removal vs. experimental run, (b) predicted and experimental COD removal vs. experimental run.

### 3.4. Analysis of Variance and Fit Summary

The analysis of variance (ANOVA) is a tool which presents descriptive statistics and statistical tests. ANOVA interprets complicated relationship between independent and dependent factors of complete data. The results are assessed using different statistical analysis and tests, such as alpha (0.05) at 5%, probability (*p*-value) at 95% confidence level and Fisher' test (F-test). Typically for higher F-values (greater than 4.0) and lower *p*-values (less than 0.05), ANOVA table identifies the parameter's significance in the model. In this study the results obtained from ANOVA indicated that all four independent factors and their interactions were substantial and significantly influenced the removal of PAHs and COD. The higher F-values of PAHs (16.87) and COD (37.86) models showed that both models were significant. Likewise, *p*-values of both models were less than 0.05, which confirmed significance of both models. Thus, these values are acceptable and all independent parameters have a significant impact on models.

Furthermore, coefficient of determination ( $R^2$ ) for PAHs and COD were 0.94 and 0.97, respectively which displayed reliability in PAHs and COD removal estimation. The higher values of  $R^2$  exhibited a good relationship between predicted and observed values [49]. Adequate precision (AP) for PAHs and COD removal efficiency were found 15.07% and 17.7%, respectively which showed adequate signal. The predicted and experimental values of responses models correlated with each other and indicated a significant agreement as shown in Figures 4 and 5, where a linear behavior has been demonstrated by plots which suggest that prediction of the models was accurate.

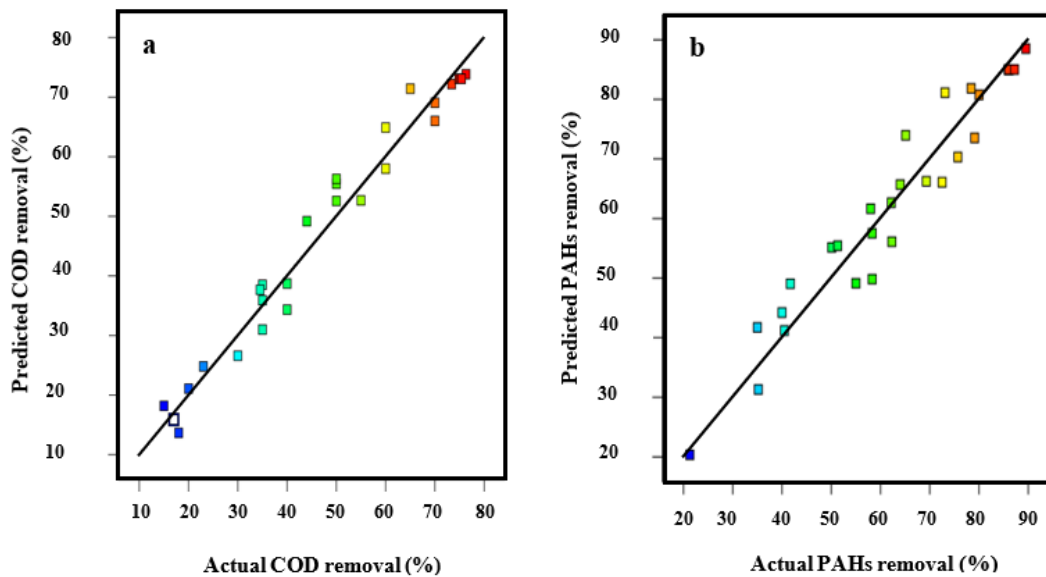


Figure 4. Predicted vs. actual removal (%); (a) COD removal, and (b) PAHs removal.

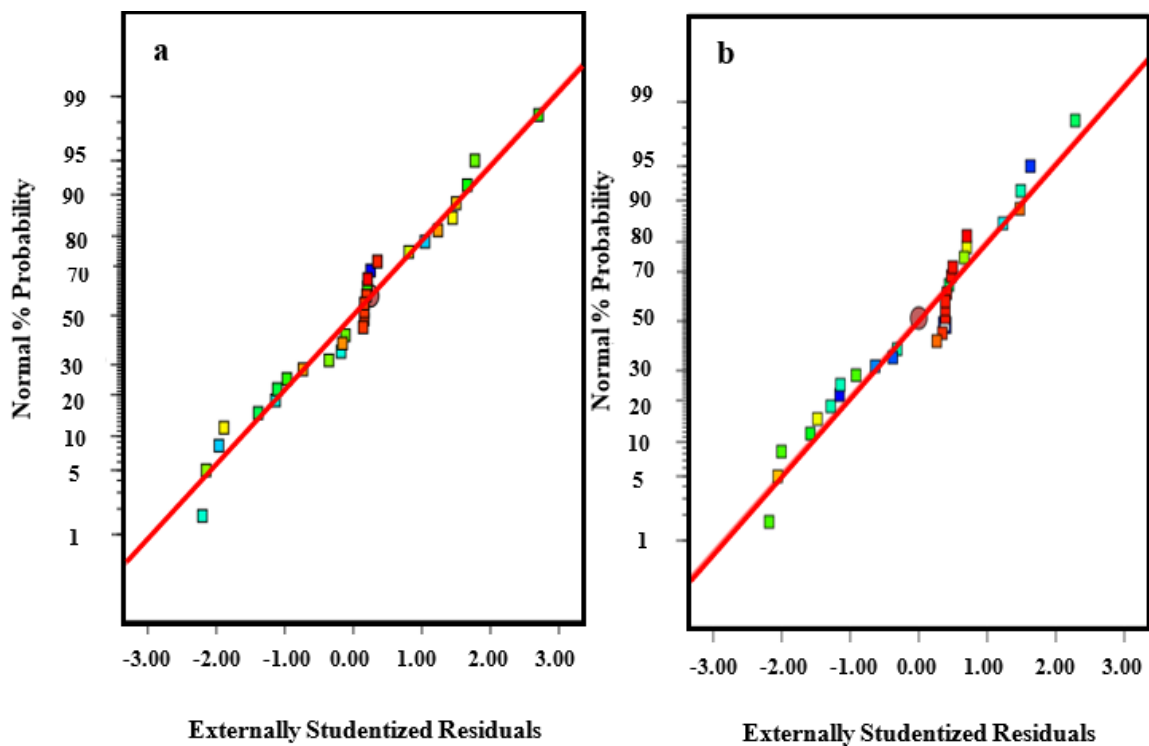
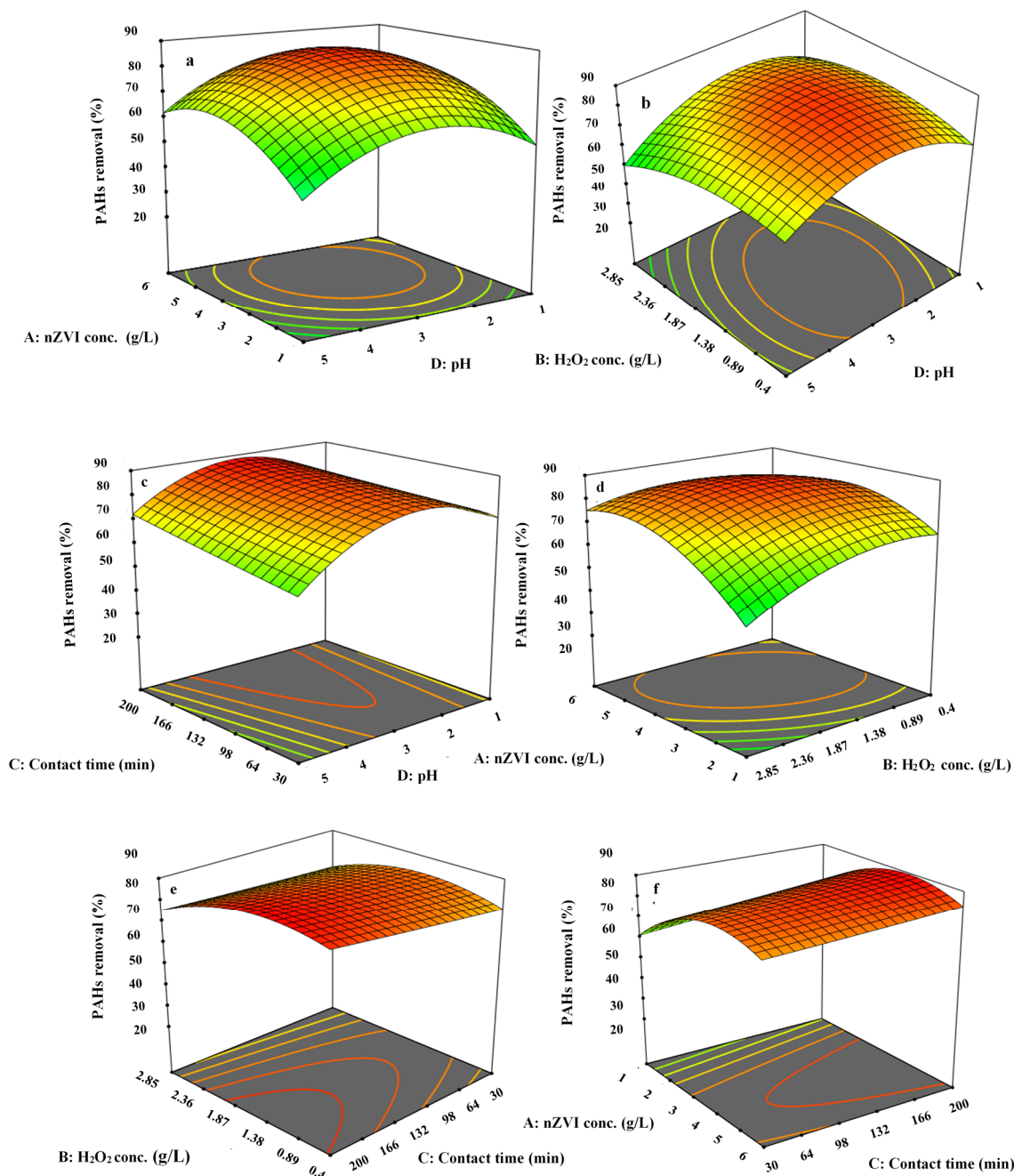


Figure 5. Normal percentage probability plot of residuals for (a) PAHs removal and (b) COD removal.

### 3.5. 3-Dimensional Surface Plots for PAHs and COD Removal Efficiency

3D plots carrying different peak values and curves represent the impact of independent variables and their interaction on PAHs and COD removal. In 3D plots, two independent variables were systematically varied while keeping other independent variables fixed. The most promising results of PAHs and COD removal efficiencies were chosen as shown in Figures 6 and 7, respectively.



**Figure 6.** PAHs removal (%) 3D plot; (a) nZVI dosage vs. pH, (b) H<sub>2</sub>O<sub>2</sub> conc. vs. pH (c), contact time vs. pH, (d) nZVI dosage vs. H<sub>2</sub>O<sub>2</sub>, (e) H<sub>2</sub>O<sub>2</sub> conc. vs. contact time, (f) nZVI vs. contact time.

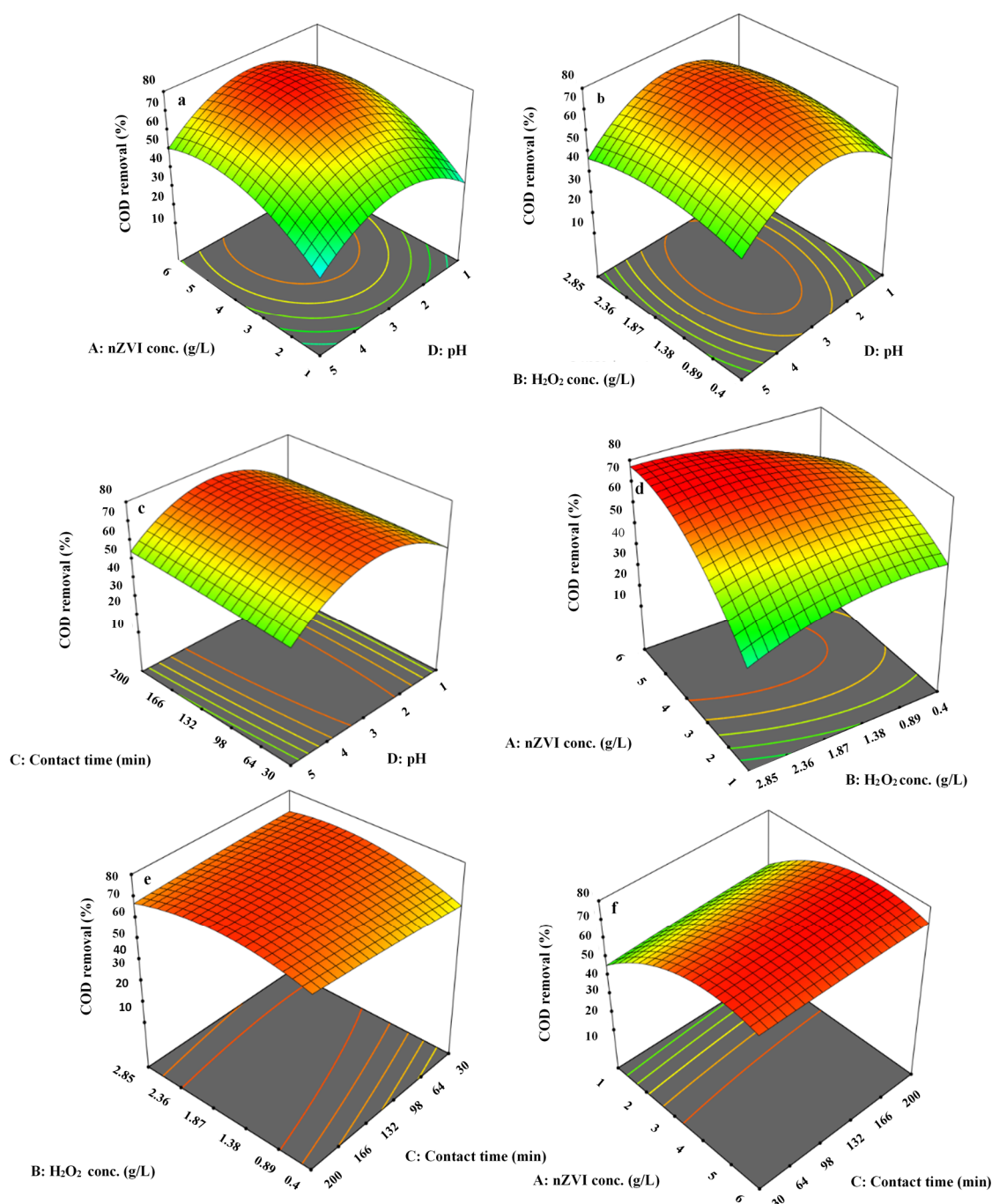


**Figure 7.** COD removal (%) 3D plot; (a) nZVI dosage vs. pH, (b) H<sub>2</sub>O<sub>2</sub> conc. vs. pH (c), contact time vs. pH, (d) nZVI dosage vs. H<sub>2</sub>O<sub>2</sub> (e), H<sub>2</sub>O<sub>2</sub> conc. vs. contact time, (f) nZVI vs. contact time.

The impact of pH on PAHs and COD removal efficiencies is shown in Figures 6a–c and 7a–c, respectively. In Figures 6 and 7 it can be seen that by increasing the pH value up to a certain value has a positive influence on PAHs and COD removal efficiencies. While varying the pH value above optimum value have negative impact on removal efficiencies. In these Figures, nZVI concentration, H<sub>2</sub>O<sub>2</sub> concentration, and contact time were kept fixed at 3.0 g/L, 1.38 g/L and 120 min, in turn. Initially at pH of 1.0, the PAHs removal efficiencies were 73.0%, 74.2% and 74.5%, whereas, COD removal efficiencies were 54.2%, 55.7% and 56.5%. An increment in organic removal was found as the value of pH was increased from 1.0 to 3.0. Further, at pH 2.0 the PAHs removal efficiencies surged up to 78.5%, 79.4% and 81.2% (Figure 6). Similarly, COD removal efficiencies followed the same trend for

pH 2.0 and increased up to 58.3%, 59.7% and 61.7% (Figure 7). Likewise, at pH 3.0, PAHs removal efficiencies increased up to 83.4%, 85.8%, and 85.2% (Figure 6). Similarly COD removal increased up to 70.3%, 72.0%, and 73.2% (Figure 7). The removal efficiencies trend started to decline as the pH value was increased beyond pH 3.0. pH of the aqueous solution is a very important parameter that controls the production of  $\text{Fe}^{2+}$  and  $\text{OH}^\bullet$  during the reaction. In both Figures 6a–c and 7a–c pH below 3.0 decreases the PAHs and COD degradation due to the generation of complex Fe species and oxonium ions ( $\text{H}_3\text{O}^+$ ). The pH values above pH 3.0 may inhibit the hydrogen peroxide decomposition due to the absence of  $\text{H}^+$  ions and therefore decrease the formation of  $\text{OH}^\bullet$  radical, which may decrease the removal efficiencies of PAHs and COD above pH 3.0.

Besides, at higher pH value of aqueous solution,  $\text{Fe}^{3+}$  converts into  $\text{Fe}(\text{OH})_3$  in the form of precipitate, which hinders the generation of  $\text{Fe}^{2+}$  [50]. While at pH 3.0, nZVI/ $\text{H}_2\text{O}_2$  generates a higher amount of  $\text{Fe}^{2+}$  and  $\text{OH}^\bullet$  ions, which are the main ions for the degradation of organic pollutants in produced water. Shafieiyoun et al. [33] reported that the increase in pH above 3.0 decreases  $\text{OH}^\bullet$  oxidation potential. Similar results have been reported by other researchers showing pH 3.0 as optimal value for heterogeneous Fenton like oxidation system using nZVI as catalyst for maximum removal of organic pollutants [51]. Yaqub et al. [52] reported that highest PAHs degradation was attained at pH 3.0 in produced water. Viardi et al. [53] achieved maximum COD removal efficiency from tannery wastewater at pH 3.0. Similarly, Yu et al. [50] reported pH 3.0 as the optimum value for maximum removal of organic pollutants. In another study, Kallel et al. [54] found that acidic medium (between pH 2.0–4.0) is favorable for the production of  $\text{Fe}^{2+}$  and  $\text{OH}^\bullet$  which are primary ions for elimination of carbon-based pollutants from wastewater. The effect of  $\text{H}_2\text{O}_2$  concentrations on PAHs and COD removal has been shown at pH 4.0 (Figures 6b and 7b), and 166 min of contact time (Figures 6e and 7e), respectively. Initially, at 0.40 g/L concentration of  $\text{H}_2\text{O}_2$ , the PAHs reduction efficiencies were 78.6% and 84.0%, while COD removals were about 60.0% and 67.1%. In addition, 3D plots showed that increase in the concentration of  $\text{H}_2\text{O}_2$  from 0.40 g/L to 1.87 g/L improved PAHs and COD removal efficiencies. It was observed that the value of PAHs removal efficiencies surged up to 80.3% and 85.1% at 1.38 g/L dosage of  $\text{H}_2\text{O}_2$  (Figure 6). Similarly, COD removal efficiencies were improved from 60.0% to 70.0% (Figure 7). Moreover, the increment in PAHs and COD removal efficiencies were reached up to their maximum values 87.0% and 75.3%, respectively, at 1.87 g/L concentration of  $\text{H}_2\text{O}_2$  (Figures 6 and 7). Further increases (beyond 1.87 g/L) in  $\text{H}_2\text{O}_2$  concentration decreased the removal efficiencies of PAHs and COD. The influence of  $\text{H}_2\text{O}_2$  concentration can be illustrated by reaction of  $\text{H}_2\text{O}_2$  and  $\text{Fe}^{2+}$  ions. As concentration of  $\text{H}_2\text{O}_2$  increased, it generated a larger amount of  $\text{OH}^\bullet$  by reacting with  $\text{Fe}^{2+}$  increasing removal efficiency of organic pollutants [35]. The effect of  $\text{H}_2\text{O}_2$  concentration on PAHs and COD removal depends on the dosage of nZVI also. An excessive amount of  $\text{H}_2\text{O}_2$  in the solution can cause  $\bullet\text{OH}$  scavenging effect and produces hydroperoxy radical ( $\bullet\text{HO}_2$ ) which have less oxidation potential than  $\text{OH}^\bullet$  as given in Equation (18) [43]. Few studies have reported approximately 1.87 g/L of  $\text{H}_2\text{O}_2$  concentration as optimum value for maximum removal of organic pollutants from different types of wastewater which is in line with our findings [20,35]. Taha et al. [24] reported similar results, and they obtained a maximum 75.0% removal of organic pollutants from palm oil mill wastewater at 1.84 g/L of  $\text{H}_2\text{O}_2$  concentration. Bogacki et al. [20] achieved highest organic pollutant removal (76.0%) from wastewater at 1.90 g/L concentration of  $\text{H}_2\text{O}_2$ .



The effect of nZVI dosage on PAHs and COD degradation was noticeable as shown in Figure 6a,f and Figure 7a,f, respectively. When nZVI dosage was increased from 1.0–6.0 g/L at pH 2.0 and 90 min of contact time, PAHs and COD removal varied accordingly. Figures 6a and 7a depicts that at 1.0 g/L of nZVI dosage PAHs and COD removal were 65.6% and 45.3%, respectively. The PAHs and COD removal efficiencies surged by increasing the concentration of nZVI from 1.0 g/L until 4.0 g/L. At 4.0 g/L concentration of nZVI, the removal efficiencies of PAHs and COD were 84.0% and 71.0%, respectively (Figures 6a and 7a). However, beyond 4.0 g/L of nZVI, PAHs and COD removal started to decrease.

At 6.0 g/L of nZVI, removal of PAHs and COD were 79.0% and 68.3%, respectively (Figures 6a and 7a). In Figures 6f and 7f, similar trends were followed by nZVI concentration for PAHs and COD removal efficiencies, respectively. At 1.0 g/L dosage of nZVI, the PAHs and COD removal efficiencies were at their minimum level, 60.1% and 45.5% respectively. The reduction of PAHs and COD increased as the dosage of nZVI was increased from 1.0 to 4.0 g/L. At 4.0 g/L of nZVI concentration the PAHs and COD elimination reached up to 70.3% and 55.8%, respectively. In addition, the removal efficiencies of PAHs and COD declined as the concentration of nZVI was increased beyond 4.0 g/L. At initial concentration of nZVI (1.0 g/L), less amount of  $\text{Fe}^{2+}$  was produced but as the nZVI concentration increased, the amount of  $\text{Fe}^{2+}$  also increased, more sites were available, which favored the higher generation of  $\text{OH}^\bullet$  [26]. This phenomenon enhanced removal of organic contaminants. Nevertheless, increase in nZVI concentration beyond optimum value releases more  $\text{Fe}^{2+}$  ions in aqueous solution that may cause scavenging of  $\text{OH}^\bullet$  by formation of  $\text{Fe}_2\text{O}_3$  and  $\text{OH}^-$  and these oxides passivate on the surface of nZVI as shown in Equation (19) [55]. The  $\text{Fe}^{2+}$  ions may replace the pollutants present in aqueous solution and react with  $\text{OH}^\bullet$  instead of organic compounds, which causes reduction of organic pollutants degradation at higher concentrations of nZVI.



Several researchers have reported optimum value of nZVI concentration for maximum removal of organic pollutants is equal or close to 4.0 g/L [35]. Bogacki et al. [20] obtained maximum organic pollutants removal from automotive wastewater at 4.0 g/L of nZVI concentration. Taha et al. [45], reported 3.91 g/L of nZVI concentration as optimum value for maximum removal of organic pollutants, and they achieved highest removal (75%) of organic pollutants. The best PAHs and COD reduction efficiencies were obtained in the range of 60.0–89.5%, and 40.0–76.3%, respectively, which is based on significant interaction between four input factors. In this study, higher removal of PAHs and COD was obtained using heterogeneous Fenton like oxidation system as compared to previously reported studies [18,35,54,56,57]. Some studies used synthetic wastewater and have reported higher removal of organics than the current work. However, in synthetic wastewater just a certain amount of targeted organic pollutants are added, and reagents do attack only on targeted organic contaminants rather than on other unwanted compounds [58,59], as shown in Table 4.

**Table 4.** Comparison of previously conducted heterogeneous Fenton like oxidation studies with the current study.

Method	Type of Effluents	Pollutants	Removal (%)	References
nZVI/H <sub>2</sub> O <sub>2</sub>	Synthetic wastewater	Polyvinyl alcohol	94.0	[55]
nZVI/H <sub>2</sub> O <sub>2</sub>	Synthetic wastewater	pentachlorophenol	57.0	[56]
nZVI/H <sub>2</sub> O <sub>2</sub>	Tannery wastewater	COD	75.5	[57]
nZVI/H <sub>2</sub> O <sub>2</sub>	Synthetic wastewater	Benzotriazole and COD	73.4 and 40.0	[58]
nZVI/H <sub>2</sub> O <sub>2</sub>	Synthetic wastewater	Amoxicillin and COD	86.5 and 71.2	[11]
nZVI/H <sub>2</sub> O <sub>2</sub>	Contaminated soil	PAHs	80.0	[52]
nZVI/H <sub>2</sub> O <sub>2</sub>	Tannery wastewater	TOC, COD and phenol	70.0, 73.0 and 88.0	[59]
nZVI/H <sub>2</sub> O <sub>2</sub>	Landfill Leachate	COD	74.0	[60]
nZVI/H <sub>2</sub> O <sub>2</sub> /microwave irradiation	Landfill Leachate	Organic compounds	58.0	[61]
nZVI/H <sub>2</sub> O <sub>2</sub> /biodegradation	Synthetic wastewater	COD and naphthalene	55.2 and 99.0	[47]
nZVI/H <sub>2</sub> O <sub>2</sub>	Produced water	COD and PAHs	76.3 and 89.5	This Study

### 3.6. Optimization and Validation of Experimental Study

Optimal values for every individual experiment (response) is considered very hard to obtain. Therefore, numerical optimization is the best option to get optimal values. Numerical optimization is RSM based technique which is usually applied after ANOVA model validation to find the optimal conditions of all independent variables for desired removal percentage of responses. It also predicts removal percentage of responses based on proposed optimal values of independent variables which need to be validated by conducting an additional experiment [59]. The principle of this optimization is based on desirability function and comprehensive explanation of desirability function has been

explained by X.Y. Shi et al. [62]. For this purpose “numerical optimization” based on quadratic models (Equations (16) and (17)) and the parameters in their critical ranges were practiced. For numerical optimization of operating conditions for the current study, “in range” options were selected for independent variables (nZVI concentration, H<sub>2</sub>O<sub>2</sub> concentration, contact time and pH) while for PAHs and COD removal “maximize” options were chosen. The PAHs and COD removal efficiencies predicted by numerical optimization were 89.38% and 75.74%, respectively. Besides, these removal efficiencies were predicted at the optimum values of all four-independent variables such as nZVI (4.35 g/L), H<sub>2</sub>O<sub>2</sub> (1.60 g/L), contact time (199.9 min) and pH (2.94).

For the validation of optimal conditions and the entire model an additional experiment was performed using the proposed optimal values of independent parameters. The responses obtained from experiment were same as the models predicted with a slight difference. The removal efficiencies of PAHs and COD gained from the experiment at predicted optimal conditions were 87.4% and 73.5%, respectively. There was a minor difference between predicted and experimental results at the optimal conditions which verified the model validity. Besides, all HMW PAHs were removed entirely, while it partially removed LMW PAHs such as naphthalene, acenaphthylene, acenaphthene, and fluorene. The concentration of naphthalene, acenaphthylene, acenaphthene, and fluorene after the treatment of produced water at optimal conditions were 64.13 µg/L, 30 µg/L, 42.23 µg/L, and 23.21 µg/L, respectively, as shown in Figure 8.

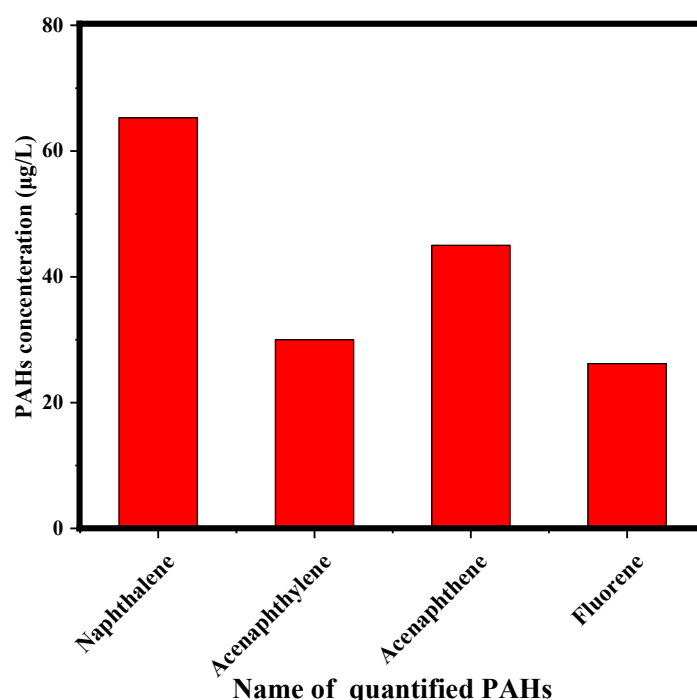


**Figure 8.** Concentration of PAHs in produced water after optimization of heterogeneous Fenton like oxidation system.

This shows that these LMW PAHs were more stable and resistant against the heterogeneous Fenton like oxidation system than the HMW PAHs. The small difference between predicted and experimental values indicated that CCD design is a useful tool to obtain the best optimal conditions for maximum PAHs and COD removal from produced water.

In summary, a heterogeneous Fenton like oxidation system using nZVI as a catalyst was utilized for the removal of PAHs and COD from produced water. Design-Expert software was practiced to investigate the optimal conditions of four independent variables with significant *p*-values of PAHs and COD models (<0.05). In the validation experiment, there was a minor difference between predicted and experimental values, which indicated that the model was significant. The maximum removal of

PAHs and COD at optimal conditions was 87.4% and 73.5%, respectively. Interestingly, real produced water was utilized and all experiments were performed at lab scale in current study. Based on the excellent results of heterogeneous Fenton like oxidation system obtained for the treatment of PW, it is expected that this system can efficiently treat PW in a bench scale setup. Therefore, in future, this system can be extended in a bench scale reactor built according to full scale plant configuration for the treatment of real produced water. Furthermore, the obtained optimized operating conditions from bench scale reactor could be employed for full-scale plant.

#### 4. Conclusions

This study investigated heterogeneous Fenton like system using nZVI as a catalyst for removal of organic and inorganic carbon pollutant from real produced water. Independent variables were studied via preliminary experiments and then used in RSM optimization for the removal of PAHs and COD. RSM based CCD was used to design the experimental sets. CCD developed total 30 experimental runs with different values of four independent variables. Experimental conditions were optimized using numerical optimization in CCD/RSM to achieve highest removal of PAHs and COD. The optimal values were 4.35 g/L of nZVI and 1.60 g/L of H<sub>2</sub>O<sub>2</sub> at reaction time of 199.90 min and 2.94 pH. The maximum predicted values of PAHs and COD removal at optimal conditions were 89.3% and 75.7%, respectively. While experimental values of PAHs and COD removal were 87.4% and 73.5%, respectively. The small error between predicted and experimental responses confirms validation of the designed model. All HMW PAHs were removed completely, whereas, LMW PAHs such as naphthalene, acenaphthylene, acenaphthene, and fluorene were partially removed. Based on obtained results, heterogeneous Fenton like oxidation system using nZVI as a catalyst is presented as promising method for the treatment of produced water, which can be extended to the removal of other micropollutants such as Endocrine-disrupting chemicals (EDCs), and pharmaceuticals.

**Author Contributions:** Conceptualization, M.R.U.M., K.R. and Y.C.H.; data curation, T.H.; Formal analysis, K.R.; funding acquisition, M.R.U.M.; investigation, T.H. and K.R.; methodology, T.H.; project administration, M.R.U.M.; resources, M.R.U.M.; supervision, M.R.U.M. and K.R.; validation, K.R.; writing—original draft, T.H.; writing—review and editing, M.R.U.M., K.R. and S.R.M.K. All authors have read and agreed to the published version of the manuscript.

**Funding:** This research was funded by YUTP research project (Cost center 015LC0-044).

**Acknowledgments:** The financial support provided by Universiti Teknologi PETRONAS under YUTP research project (Cost center 015LC0-044) is highly appreciated. Graduate Assistantship scheme by the Centre for Graduate Studies of Universiti Teknologi PETRONAS (UTP) is much appreciated. Additionally, the authors also appreciate the effort of Qatar National Library (QNL) for sponsoring the publication fees of this manuscript.

**Conflicts of Interest:** The authors declare no conflict of interest.

#### References

1. Afzal, T.; Isa, M.H.; Ul Mustafa, M.R. Removal of organic pollutants from produced water using Fenton oxidation. In Proceedings of the E3S Web of Conferences, Penang, Malaysia, 18 September 2018; p. 02035.
2. Haneef, T.; Mustafa, M.R.; Farhan Yasin, H.; Farooq, S.; Hasnain Isa, M.J.E. Study of Ferrate (VI) oxidation for COD removal from wastewater. *IOP Conf. Ser. Earth Environ. Sci.* **2020**, *442*, 012007. [[CrossRef](#)]
3. Igunnu, E.T.; Chen, G.Z. Produced water treatment technologies. *Int. J. Low Carbon Technol.* **2014**, *9*, 157–177. [[CrossRef](#)]
4. Akinpelu, A.A.; Ali, M.E.; Johan, M.R.; Saidur, R.; Qurban, M.A.; Saleh, T.A. Polycyclic aromatic hydrocarbons extraction and removal from wastewater by carbon nanotubes: A review of the current technologies, challenges and prospects. *Process. Saf. Environ. Prot.* **2019**, *122*, 68–82. [[CrossRef](#)]
5. Yaqub, A.; Isa, M.H.; Ajab, H.; Kutty, S.R.; Ezechi, E.H. Polycyclic aromatic hydrocarbons removal from produced water by electrochemical process optimization. *Ecol. Chem. Eng. S* **2017**, *24*, 397–404. [[CrossRef](#)]
6. Fakhru, R.A.; Pendashteh, A.; Abdullah, L.C.; Biak, D.R.A.; Madaeni, S.S.; Abidin, Z.Z. Review of technologies for oil and gas produced water treatment. *J. Hazard. Mater.* **2009**, *170*, 530–551.



7. Rasool, K.; Shahzad, A.; Lee, D.S. Exploring the potential of anaerobic sulfate reduction process in treating sulfonated diazo dye: Microbial community analysis using bar-coded pyrosequencing. *J. Hazard. Mater.* **2016**, *318*, 641–649. [[CrossRef](#)]
8. Saeed, M.O.; Azizli, K.; Isa, M.H.; Bashir, M.J. Application of CCD in RSM to obtain optimize treatment of POME using Fenton oxidation process. *J. Water Process. Eng.* **2015**, *8*, 7–16. [[CrossRef](#)]
9. Gautam, P.; Kumar, S.; Lokhandwala, S. Advanced oxidation processes for treatment of leachate from hazardous waste landfill: A critical review. *J. Clean. Prod.* **2019**, *237*, 1–14. [[CrossRef](#)]
10. Nawaz, M.; Shahzad, A.; Tahir, K.; Kim, J.; Moztahida, M.; Jang, J.; Alam, M.B.; Lee, S.H.; Jung, H.Y.; Lee, D.S. Photo-Fenton reaction for the degradation of sulfamethoxazole using a multi-walled carbon nanotube-NiFe<sub>2</sub>O<sub>4</sub> composite. *Chem. Eng. J.* **2020**, *382*, 123053. [[CrossRef](#)]
11. Zha, S.; Cheng, Y.; Gao, Y.; Chen, Z.; Megharaj, M.; Naidu, R. Nanoscale zero-valent iron as a catalyst for heterogeneous Fenton oxidation of amoxicillin. *Chem. Eng. J.* **2014**, *255*, 141–148. [[CrossRef](#)]
12. Xu, L.; Wang, J. A heterogeneous Fenton-like system with nanoparticulate zero-valent iron for removal of 4-chloro-3-methyl phenol. *J. Hazard. Mater.* **2011**, *186*, 256–264. [[CrossRef](#)] [[PubMed](#)]
13. Jarosova, B.; Filip, J.; Hilscherová, K.; Tuček, J.; Šimek, Z.; Giesy, J.P.; Zbořil, R.; Bláha, L. Can zero-valent iron nanoparticles remove waterborne estrogens? *J. Environ. Manag.* **2015**, *150*, 387–392. [[CrossRef](#)] [[PubMed](#)]
14. Zhao, X.; Liu, W.; Cai, Z.; Han, B.; Qian, T.; Zhao, D. An overview of preparation and applications of stabilized zero-valent iron nanoparticles for soil and groundwater remediation. *Water Res.* **2016**, *100*, 245–266. [[PubMed](#)]
15. Zhang, W.; Gao, H.; He, J.; Yang, P.; Wang, D.; Ma, T.; Xia, H.; Xu, X. Removal of norfloxacin using coupled synthesized nanoscale zero-valent iron (nZVI) with H<sub>2</sub>O<sub>2</sub> system: Optimization of operating conditions and degradation pathway. *Sep. Purif. Technol.* **2017**, *172*, 158–167. [[CrossRef](#)]
16. He, J.; Yang, X.; Men, B.; Wang, D.J. Interfacial mechanisms of heterogeneous Fenton reactions catalyzed by iron-based materials: A review. *Int. J. Environ. Sci.* **2016**, *39*, 97–109. [[CrossRef](#)]
17. Zhang, W.X. Nanoscale iron particles for environmental remediation: An overview. *J. Nanopart. Res.* **2003**, *5*, 323–332. [[CrossRef](#)]
18. Lee, J.H.; Park, S.Y.; Lee, B.H. Removal of Ethanolamine (ETA) and COD produced in a power plant wastewater by nano-ZVI (zerovalent iron) and hydrogen peroxide (H<sub>2</sub>O<sub>2</sub>). *Int. J. Environ. Sci.* **2019**, *10*, 62–65. [[CrossRef](#)]
19. Crane, R.A.; Scott, T.B.; Engineering, J.J. Nanoscale zero-valent iron: Future prospects for an emerging water treatment technology. *J. Hazard. Mater.* **2012**, *211*, 112–125. [[CrossRef](#)]
20. Bogacki, J.; Hazmi, H. Automotive fleet repair facility wastewater treatment using air/ZVI and air/ZVI/H<sub>2</sub>O<sub>2</sub> processes. *Arch. Environ. Prot.* **2017**, *43*, 24–31. [[CrossRef](#)]
21. Vilar, G.; Sebastiani, D.; Miliziano, S.; Verdonesi, N.; Di Palma, L. Heterogeneous nZVI induced Fenton oxidation process to enhance biodegradability of excavation by products. *Chem. Eng. J.* **2018**, *335*, 309–320. [[CrossRef](#)]
22. Kempthorne, O. *The Design and Analysis of Experiments*; American Psychological Association: Washington, DC, USA, 1952.
23. Ahmad, A.; Ismail, S.; Bhatia, S. Optimization of coagulation– flocculation process for palm oil mill effluent using response surface methodology. *Environ. Sci. Technol.* **2005**, *39*, 2828–2834. [[CrossRef](#)] [[PubMed](#)]
24. Taha, M.R.; Ibrahim, A.H. COD removal from anaerobically treated palm oil mill effluent (AT-POME) via aerated heterogeneous Fenton process: Optimization study. *J. Water Process. Eng.* **2014**, *1*, 08–16. [[CrossRef](#)]
25. Mahmoud, A.S.; El-Tayieb, M.M.; Ahmed, N.A.S.; Mostafa, A.M. Algorithms and statistics for municipal wastewater treatment using nano zero valent iron (nZVI). *J. Environ. Biotechnol.* **2018**, *7*, 30–44.
26. Rice, E.W.; Baird, R.B.; Nikazar, M. *Standard Methods for the Examination of Water and Wastewater*; American Public Health Association: Washington, DC, USA, 2005; Volume 4.
27. Taha, M.R.; Ibrahim, A.H. Characterization of nano zero-valent iron (nZVI) and its application in sono-Fenton process to remove COD in palm oil mill effluent. *J. Environ. Chem.* **2014**, *2*, 1–8. [[CrossRef](#)]
28. Giasuddin, A.B.; Kanel, S.R.; Choi, H. Technology. Adsorption of humic acid onto nanoscale zerovalent iron and its effect on arsenic removal. *Environ. Sci. Technol.* **2007**, *41*, 2022–2027. [[CrossRef](#)] [[PubMed](#)]
29. Li, X.Q.; Elliott, D.W.; Zhang, W.X. Zero-valent iron nanoparticles for abatement of environmental pollutants: Materials and engineering aspects. *Crit. Rev. Solid State* **2006**, *31*, 111–122. [[CrossRef](#)]

30. Sun, Y.P.; Li, X.Q.; Cao, J.; Zhang, W.X.; Wang, H.P. Characterization of zero-valent iron nanoparticles. *Adv. Colloid Interface Sci.* **2006**, *120*, 47–56. [[CrossRef](#)]
31. Kang, Y.G.; Yoon, H.; Lee, W.; Kim, E.J.; Chang, Y.S. Comparative study of peroxide oxidants activated by nZVI: Removal of 1-, 4-Dioxane and arsenic(III) in contaminated waters. *Int. J. Chem. Eng.* **2018**, *334*, 2511–2519. [[CrossRef](#)]
32. Shafieiyoun, S.; Ebadi, T.; Nikazar, M. Treatment of landfill leachate by Fenton process with nano sized zero valent iron particles. *Int. J. Environ. Sci.* **2012**, *6*, 119–128.
33. Rasool, K.; Woo, S.H.; Lee, D.S. Simultaneous removal of COD and Direct Red 80 in a mixed anaerobic sulfate-reducing bacteria culture. *Chem. Eng. J.* **2013**, *223*, 611–616. [[CrossRef](#)]
34. Singa, P.K.; Isa, M.H.; Ho, Y.C.; Lim, J.W. Mineralization of Hazardous Waste Landfill Leachate Using Photo-FENTON Process. In *E3S Web Conference*; EDP Sciences: Les Ulis, France, 2018; p. 05012.
35. Valentukeviciene, M.; Bagdziunaite, L.L.; Chadyšas, V.; Litvinaitis, A.J.S. Evaluating the impacts of integrated pollution on water quality of the trans-boundary neris (viliya) river. *Sustainability* **2018**, *10*, 4239. [[CrossRef](#)]
36. Ling, L.; Zhang, D.; Fang, J. A novel Fe(II)/citrate/UV/peroxymonosulfate process for micropollutant degradation: Optimization by response surface methodology and effects of water matrices. *Chemosphere* **2017**, *184*, 417–428. [[CrossRef](#)] [[PubMed](#)]
37. Chua, S.; Malek, M.; Chong, F. Red Lentil (*Lens culinaris*) extract as a novel natural coagulant for turbidity reduction: An evaluation, characterization and performance optimization study. *Water* **2019**, *11*, 1686. [[CrossRef](#)]
38. Chua, S.; Chong, F.; Yen, C. Valorization of conventional rice starch in drinking water treatment and optimization using response surface methodology (RSM). *Chem. Eng. Commun.* **2019**, 1–11. [[CrossRef](#)]
39. Wei, W.; Han, X.; Zhang, M.; Zhang, Y.; Zheng, C.J.I.J.o.B.M. Macromolecular humic acid modified nano-hydroxyapatite for simultaneous removal of Cu (II) and methylene blue from aqueous solution: Experimental design and adsorption study. *Int. J. Biol. Macromol.* **2020**, *150*, 849–860. [[CrossRef](#)] [[PubMed](#)]
40. Saeed, T.F.; Muyeed, A.A.; Ahmad, T. *Environmental Sanitation Wastewater Wreatment and Disposal*; University Grants Commission of Bangladesh: Dhaka, Bangladesh, 2014.
41. Lu, J.; Wang, X.; Shan, B.; Li, X.; Wang, W. Analysis of chemical compositions contributable to chemical oxygen demand (COD) of oilfield produced water. *Chemosphere* **2006**, *62*, 322–331. [[CrossRef](#)]
42. Aljuboury, D.A.; Palaniandy, P.H.B.; Feroz, S. Treatment of petroleum wastewater by conventional and new technologies-A review. *Glob. Nest J.* **2017**, *19*, 439–452.
43. Chowdhury, K.H.; Husain, T.; Veitch, B.; Hawboldt, K. Probabilistic risk assessment of polycyclic aromatic hydrocarbons (PAHs) in produced water. *Hum. Ecol. Risk Assess.* **2010**, *15*, 1049–1063. [[CrossRef](#)]
44. Durell, G.S.; Johnsen, S. Determining produced water originating polycyclic aromatic hydrocarbons in North Sea waters: Comparison of sampling techniques. *Mar. Pollut. Bull.* **1999**, *38*, 977–989.
45. Jagadevan, S.; Jayamurthy, M.; Dobson, P. A novel hybrid nano zerovalent iron initiated oxidation e biological degradation approach for remediation of recalcitrant waste metalworking fluids. *Water Res.* **2012**, *46*, 2395–2404. [[CrossRef](#)]
46. Joo, S.H.; Feitz, A.J.; Sedlak, D.L.; Waite, T.D. Quantification of the oxidizing capacity of nanoparticulate zero-valent iron. *Environ. Sci. Technol.* **2005**, *39*, 1263–1268. [[CrossRef](#)] [[PubMed](#)]
47. Manan, T.S.; Khan, T.; Sivapalan, S. Application of response surface methodology for the optimization of polycyclic aromatic hydrocarbons degradation from potable water using photo-Fenton oxidation process. *Sci. Total Environ.* **2019**, *665*, 196–212. [[CrossRef](#)] [[PubMed](#)]
48. Yu, B.; Jin, X.; Kuang, Y.; Megharaj, M.; Naidu, R.; Chen, Z. An integrated biodegradation and nano oxidation used for the remediation of naphthalene from aqueous solution. *Chemosphere* **2015**, *141*, 205–211. [[CrossRef](#)] [[PubMed](#)]
49. Vilardi, G.; Palma, L.D.; Verdone, N. On the critical use of zero valent iron nanoparticles and Fenton processes for the treatment of tannery wastewater. *J. Water Process. Eng.* **2018**, *22*, 109–122. [[CrossRef](#)]
50. Kallel, M.; Belaid, C.; Boussahel, R. Olive mill wastewater degradation by Fenton oxidation with zero-valent iron and hydrogen peroxide. *J. Hazard. Mater.* **2009**, *163*, 550–554. [[CrossRef](#)] [[PubMed](#)]
51. Wijesekaras, H.; Basnayake, A.; Vithanage, M. Organic-coated nanoparticulate zero valent iron for remediation of chemical oxygen demand (COD) and dissolved metals from tropical landfill leachate. *Environ. Sci. Pollut. Res.* **2014**, *21*, 7075–7087. [[CrossRef](#)]

52. Pardo, F.; Peluffo, M.; Santos, A. Optimization of the application of the Fenton chemistry for the remediation of a contaminated soil with polycyclic aromatic hydrocarbons. *J. Chem. Technol. Biot.* **2016**, *91*, 1763–1772. [[CrossRef](#)]
53. Karimi, B.; Rajaei, M.; Koulivand, A.; Cheshmeh, R. Performance evaluation of advanced  $\text{Fe}^0/\text{Fe}^{+2}/\text{Fe}^{+3}/\text{H}_2\text{O}_2$  process in the reduction of nitrate and organic matter from aqueous solution. *Desalin. Water Treat.* **2014**, *52*, 6240–6248. [[CrossRef](#)]
54. Borror, C.M.; Montgomery, D.C. Response surface design evaluation and comparison. *J. Stat. Plan. Inference* **2009**, *139*, 629–641. [[CrossRef](#)]
55. Lin, C.C.; Hsu, S.T.; Separation, J.; Technology, P. Performance of nZVI/ $\text{H}_2\text{O}_2$  process in degrading polyvinyl alcohol in aqueous solutions. *Sep. Purif. Technol.* **2018**, *203*, 111–116. [[CrossRef](#)]
56. Cheng, R.; Cheng, C.; Liu, G.H.; Zheng, X.; Li, G.; Li, J.J.C. Removing pentachlorophenol from water using a nanoscale zero-valent iron/ $\text{H}_2\text{O}_2$  system. *Chemosphere* **2015**, *141*, 138–143. [[CrossRef](#)] [[PubMed](#)]
57. Vilardi, G.; Rodríguez-Rodríguez, J.; Ochando-Pulido, J.M.; Verdone, N.; Martínez-Ferez, A.; Di Palma, L.; Protection, E. Large Laboratory-Plant application for the treatment of a Tannery wastewater by Fenton oxidation: Fe (II) and nZVI catalysts comparison and kinetic modelling. *Process. Saf. Environ. Prot.* **2018**, *117*, 629–638. [[CrossRef](#)]
58. Ahmadi, M.; Rahmani, K.; Rahmani, A.; Rahmani, H.J. Removal of benzotriazole by Photo-Fenton like process using nano zero-valent iron: Response surface methodology with a Box-Behnken design. *Pol. J. Chem. Technol.* **2017**, *19*, 104–112. [[CrossRef](#)]
59. Rezaei, F.; Vione, D. Effect of pH on Zero Valent Iron Performance in Heterogeneous Fenton and Fenton-Like Processes: A Review. *Molecules* **2018**, *23*, 3127. [[CrossRef](#)]
60. Ertugay, N.; Kocakaplan, N.; Malkoç, E. Investigation of pH effect by Fenton-like oxidation with ZVI in treatment of the landfill leachate. *Int. J. Min. Reclam. Env.* **2017**, *31*, 404–411. [[CrossRef](#)]
61. Usman, M.; Cheema, S.A.; Farooq, M.J. Heterogeneous Fenton and persulfate oxidation for treatment of landfill leachate: A review supplement. *J. Clean. Prod.* **2020**, *256*, 120448. [[CrossRef](#)]
62. Shi, X.Y.; Jin, D.W.; Sun, Q.Y.; Li, W.W. Optimization of conditions for hydrogen production from brewery wastewater by anaerobic sludge using desirability function approach. *Renew. Energy* **2010**, *35*, 1493–1498. [[CrossRef](#)]

